CHAPTER 5

DESIGN AND DEVELOPMENT OF A PROGRAMMABLE ILLUMINATION SMARTPHONE MICROSCOPY (PISM)

This chapter discusses the design and working of a multimodal microscopic platform on a smartphone for contrast enhancement of various samples using different low-cost consumer optoelectronics parts. The chapter elucidates the apprehension of seven different well-established imaging modes, namely BF, DF, OI, FI, RI, differential phase contrast (DPC), and polarized imaging (PI) on a single imaging platform. The theoretical aspects of the platform have been discussed thoroughly. The characterization by measuring different optical parameters of the proposed imaging system has been performed. At the end, the chapter discusses the performance of the developed multimodal imaging system for practical applications and compares its usability as an alternative platform over the existing commercial counterpart.

5.1 Background

Different microscopic imaging modes, such as BF, DF, FI, RI, and DPC imaging, are useful for analyzing various samples [1, 2]. For instance, colorless unstained specimens like mammalian cells do not produce much contrast under BF imaging mode. Contrast-enhancing techniques such as DF, OI, DPC, or RI are useful for such samples. Again, fluorescence microscopy provides a high specificity and sensitivity for detecting and tracking of cells, proteins, and other components in a specimen [3–5]. Usually, these methods require spatially modulated illumination systems, which can be obtained by introducing optical filters and physical masks into the condenser lens

of the microscope. For instance, in a DF microscope, a specialized opaque disc is to be inserted into the aperture focal plane of the condenser lens to create a hollow cone of light. It would produce a numerical aperture larger than the objective lens so that only the scattered light from the specimen can enter the objective lens. For RI, color filters are introduced to provide contrasting colors to the specimen against another contrasting colored background by modifying the BF and DF illumination sections. Again, for phase-contrast imaging, a phase ring is inserted into the condenser's aperture plane to fit the ring-shaped phase plate inside the objective lens [6, 7]. Though all these techniques allow direct visualization of colorless and unstained biological samples, the involvement of additional physical masks and optical filters make the system relatively complex, heavy and costly, thus makes it difficult to deploy in resource-constrained regions for point-of-care (PoC) applications.

With the availability of consumer electronic items like smartphones, Arduino microcontroller board, miniature display modules, e.g., liquid crystal displays (LCDs), OLED displays etc., opens new vista for the development of alternative, inexpensive, field-portable imaging platforms which may be useful for various applications [8–13]. In particular, the smartphone-based microscopes have proven their usability and versatility for different infield applications, which has been discussed in the previous chapters. However, most of the reported smartphone microscopes, in general, are designed to be used for a single-mode of applications such as BF, DF, or fluorescence-based imaging. Only a few works have demonstrated the realization of multimodal imaging system on the smartphone. Phillips *et al.* have demonstrated a multi-contrast microscopic system using a smartphone to generate DF, BF, and DPC images by incorporating a programmable domed LED array that illuminates the samples at different angles. The different contrast imaging modes were achieved by simultaneously synchronizing the LED illumination with the phone's camera sensor [14]. Similarly, Jung *et al.* have reported a portable multi-contrast (BF, DF, and DPC) smartphone-based microscope using an array of LEDs [15]. Kheireddine *et al.* have reported a dual-phone illumination-imaging system for the acquisition of different illumination modes such as BF, DF, and fluorescence imaging. The system comprises of two mobile phones where one has been used for illumination of the samples, and the other was used to record the images. Different illumination modes were achieved by showing different color patterns on the illumination phone [16]. Though, the use of two phones gives a versatile microscopic platform; it may introduce several drawbacks. For instance, the use of a phone to illuminate the sample makes the system bigger and costlier, and may always need to adjust the alignment of the illumination patterns with the optical axis of the camera-lens system.

Guo *et al.* and Zuo *et al.* have demonstrated a low-cost multimodal optical microscope using programmable illumination by replacing the condenser diaphragm

with an inexpensive LCD on a laboratory optical microscope [3, 7]. The backlight of the LCD was removed so that it would work as a spatial light modulator (SLM) when the optical source of the microscope is turned on [17]. By showing different patterns on the LCD, several imaging modes have been realized. In this chapter, this illumination engineering has been adapted on a miniature OLED display to develop an inexpensive, versatile, and flexible multimodal microscope on a smartphone called the PISM. The use of OLED display for the proposed PISM system serves two purposes- one as an optical source and the other as a SLM. The PISM system is designed to provide enhanced imaging with high-resolution and contrast having a relatively large FoV capability. By displaying various color and binary patterns on the OLED display, the illumination and the spatial coherence of the PISM system has been dynamically controlled. Since every pixel of the OLED emits light, it can produce a more accurate and natural color, which is desirable for a microscopic imaging. The versatility of the designed platform has been demonstrated by imaging different samples in BF, DF, OI, FI, RI, and DPC modes. Furthermore, by introducing two optical polarizers into the setup, the PISM can be converted into a polarizing microscope. The usability of different imaging modes of the PISM system has been demonstrated by imaging various samples ranging from biological to birefringence samples. The combination of these different optical imaging modalities into a single microscopic system offers several important advantages, viz. the use of multiple light sources and detectors can be obviated, and it is much less complex compared to the other multimodal imaging setup reported elsewhere [2]. Again, a single optical imaging characteristic is sometimes not sufficient to visualize a specimen that is translucent in nature. In such situations, multimodal imaging techniques can be useful for enhancing the structural and functional contrasts of a specimen. Thus, the proposed scheme of the PISM can be a turnkey solution for the development of a multimodal imaging system on a single platform which is cost-effective and performs at par with that of its commercial counterparts.

5.2 Working principle

5.2.1 The PISM

Figure 5.1 depicts the rapid prototyping of the PISM system. To ensure ease of implementation and fabrication, the PISM features a simple optical design while maintaining high-quality performance. The major components of the PISM comprise imaging optics, illumination optoelectronics, a sample holder with XYZ translational stage, and a 3D-printed housing. The optics design involved for the present imaging system is similar to the microscopic system discussed in chapter 3 and is depicted

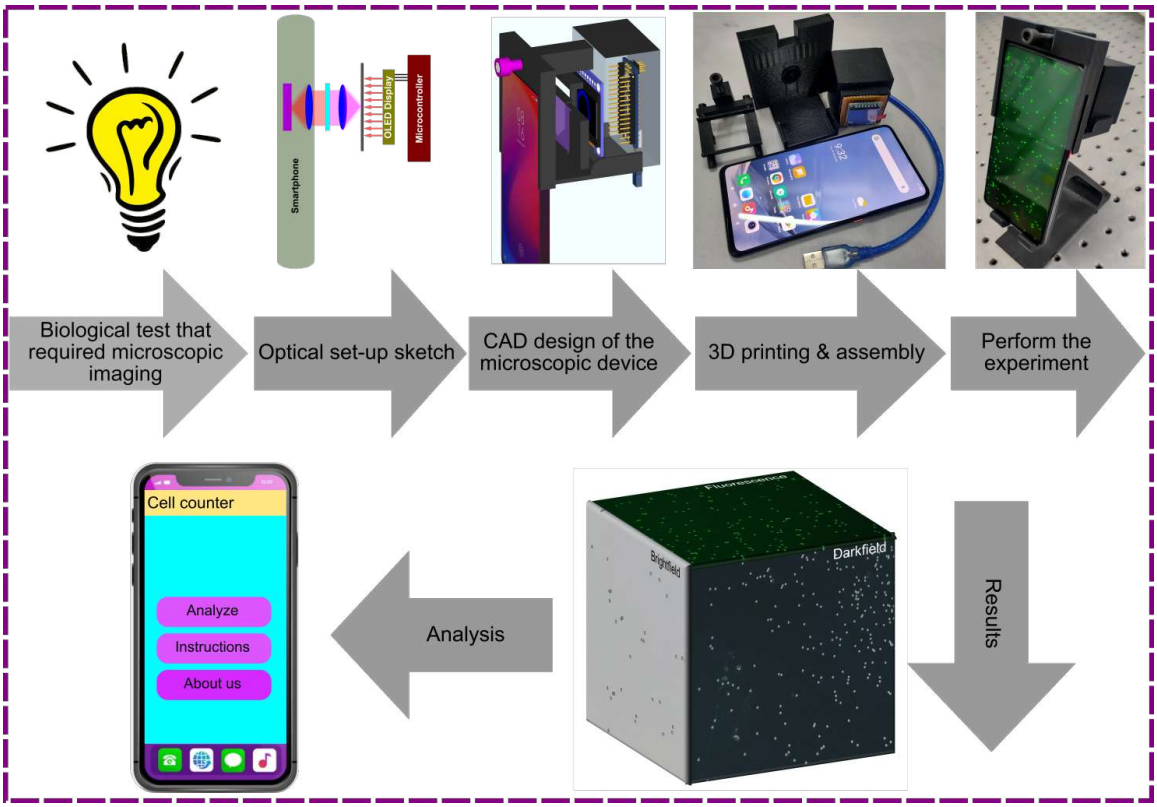

Figure 5.1: Schematic of the rapid prototyping of the PISM system.

in figure 5.2(a). The OLED display is adapted to the PISM system as an optical source. The display output of the OLED can be controlled by the phone through a microcontroller and an open-source program. The schematic of the PISM is shown in figure 5.2(c). All the components have been rigidly mounted within a 3D-printed housing, obtained from an FDM 3D printer (model: Raise N2). The sample holder is designed to hold a standard microscopic slide (75 mm x 25 mm x 1 mm) and disposable plastic hemocytometer. The 3D layout and photo image of the developed PISM system are shown in figure 5.2(d) and (e), respectively.

5.2.2 Imaging system design

For the imaging system in the present work, the $3f$ optical configuration has been implemented. This enables a relatively simple and compact implementation of the optical setup, and offers the highest acceptance for red and blue light than its $4f$ counterpart [15]. An external lens is mounted directly to the camera lens to form a finite-conjugated system. The inbuilt camera lens works as a tube lens for the $3f$ system. However, the focal length of the external lens should be small to achieve an acceptable magnification of 1 ($M \geq 1$). The imaging system consists of a Redmi K20 (Xiaomi Inc.) smartphone for image recording and analysis. This phone has a primary Sony IMX582 CMOS sensor of 48 MP with a pixel dimension of 0.8 μm

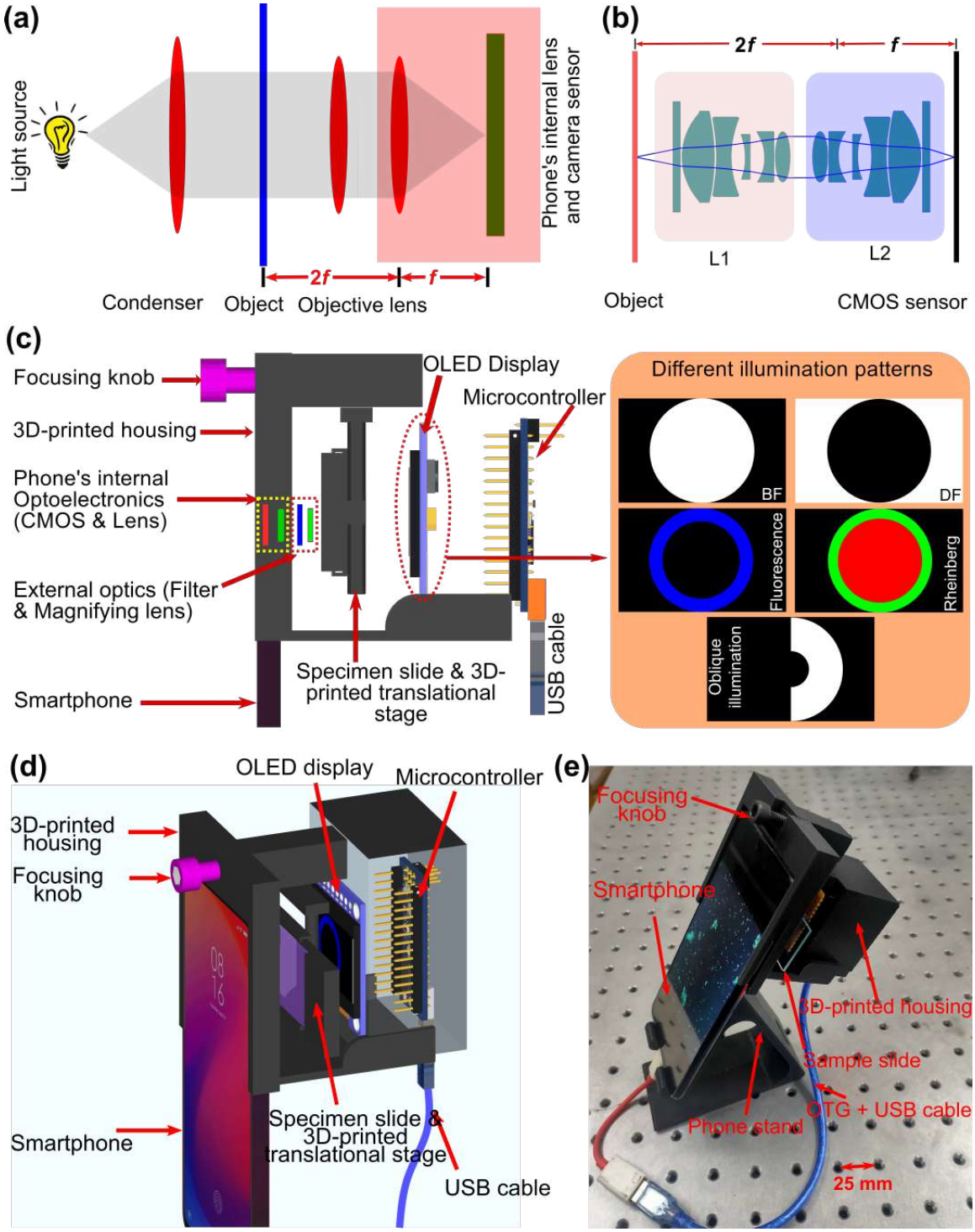

Figure 5.2: Design and fabrication of the microscopic system. (a) schematic of a $3f$ optical configuration, (b) $3f$ configuration for the present PISM system comprises of camera phone lens as an objective and the internal lens of the phone as tube lens, (c) Schematic illustration of the optical arrangement of the PISM system with different illumination patterns, (d) 3D rendering of the PISM system and (e) Prototype of the developed microscopic system.

along with a built-in lens of f-number 1.75 (focal length = 4.77 mm, back numerical aperture, NA = 0.28). In its default condition, the phone captures images with a pixel dimension of 1.6 μm (four pixels of 0.8 μm combine to form a single large pixel of 1.6 μm). Bacterial species and other pathogens have dimensions in the range of 1-5 μm. To achieve this optical resolution (r $\leq$ 1-2 μm), minimum optical magnification that would be required for the present optical setup is $M > \frac{2 \times pixel\ pitch\ of\ the\ sensor}{required\ resolution}$. Assuming the pixel pitch of the camera sensor to be 1.6 μm, an optical magnification of 3.2 would be required to obtain a resolution of 1 μm in the designed setup. One can also utilize the advantage of the camera sensor of the phone in its 48 MP imaging mode, in which case the pixel pitch is 0.8 μm and the required magnification of the objective lens to achieve the resolution of 1 μm would be 1.6 only [18].

Table 5.1: Specifications of the lenses evaluated for use as an objective lens in the PISM.

Type of Lenses	Ball lens	Achromatic doublet	iPhone 7 front camera lens
Diameter (mm)	1	4	Inner = 1.20, Outer = 4.00
Focal length (mm)	0.234	3.92	2.87
Numerical aperture	0.249	0.33	0.23
Optical magnification, M	20.38	1.22	1.66
Theoretical resolution (μm)	1.34	1.02	1.45
FOV (μm^2)	$\sim$300 $\times$ 300	$\sim$3911 $\times$ 3560	$\sim$3118 $\times$ 2452
Vendor	Edmund Optics (#43-708)	Edmund Optics (#63-714)	Amazon

Different commercially available miniature lenses with small focal lengths have been considered as a micro-objective lens for the development of the PISM. These are ball lens (Edmund Optics, part no. #43-708), achromatic doublet lens (Edmund Optics, part no. #63-714), and an iPhone7 front camera lens. Ball lens is the natural choice for the development of an inexpensive microscopic platform on mobile devices as it provides a high magnification with a little effort. For instance, 1 mm ball lens provides a magnification of 20.38 when configured to form a $3f$ imaging system. However, this lens exhibits a high aberration with small FoV thus, produces a highly distorted image due to the spherical geometry of the lens. Though, the

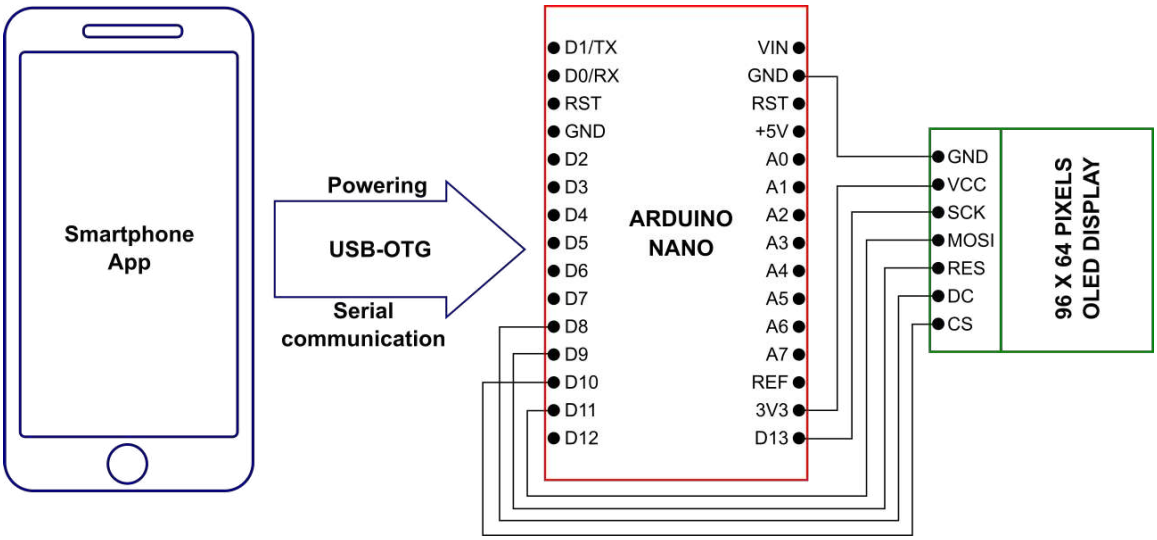

Figure 5.3: Circuit diagram for controlling the OLED display module.The OLED display has been connected to the Arduino Nano microcontroller board and established a serial communication to the smartphone app "Serial USB Terminal" via USB-OTG protocol. The USB port of the phone provides a 5V power which is sufficient to power-up the microcontroller board.

achromatic doublet lens (M = 1.22) produces better results and a larger FoV, it cannot provide the required magnification of 1.6 to resolve 1 μm objects. The iPhone 7 front camera lens on the other hand, provides superior results since it consists of multiple refractive index elements to reduce aberrations. Furthermore, this lens provides our required magnification of 1.6, thus making it possible to resolve 1 μm objects. Detailed specifications of the lenses have been provided in the table 5.1. The iPhone 7 front camera lens (FL = 2.87 mm, NA = 0.23, $f/2.2$) thus has been the choice as objective lens for the proposed PISM. The lens has been placed in the reverse orientation and aligned to the optical axis of the rear camera lens of the phone to form a 1:1.66 (object size: image size) finite-conjugated system. Figure 5.2(b) represents the schematic of the optics design for the designed PISM.

5.2.3 Illumination engineering using an OLED display

The heart of the PISM system is its illumination part. An inexpensive (USD 7.49) full color OLED display (driver IC = SSD1331, color = 65536, operating voltage = 3.3 – 5V) has been used as an illumination source for the PISM. The dimension of the display panel is 0.96 inches and has a pixel resolution of 96 × 64. An open-source smartphone application 'Serial USB Terminal', controls the intensity and the color of the display module via USB-OTG protocol with an Arduino Nano microcontroller board as an interface. The phone's internal battery powers the display panel. The circuit diagram and the detailed working of the application have been provided in the figure 5.3 and 5.4. Different color patterns have been produced by combining

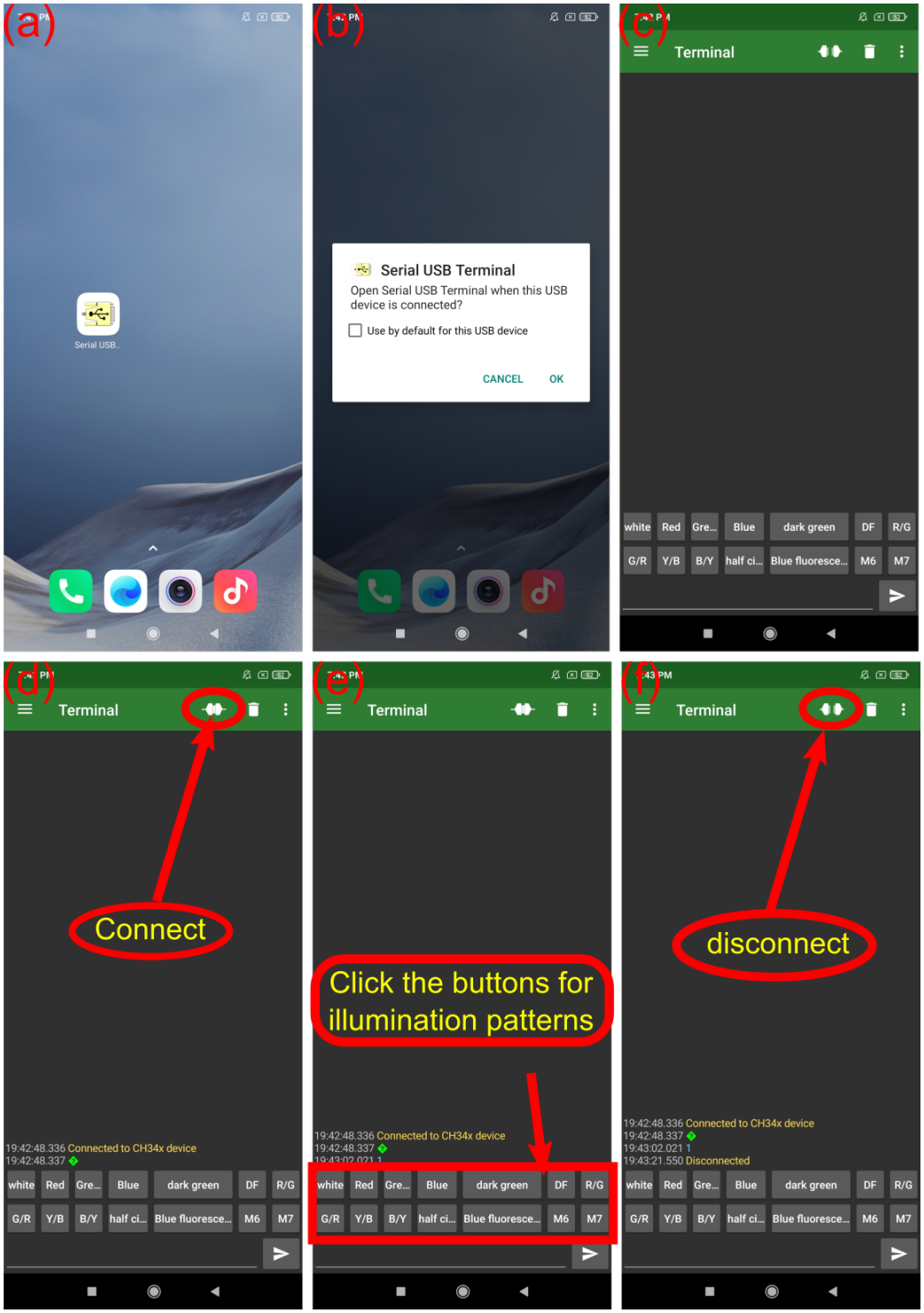

Figure 5.4: User interface (UI) and working of the open-source app “Serial USB Terminal”.(a) The app on the home screen of the phone, when the Arduino is connected via USB-OTG cable, a pop-up message appears on the screen and (c) the app will open after clicking the ‘OK’ button, (d) connect the device, (e) send data to the microcontroller to display patterns on the OLED screen, (f) disconnect the device when the task is completed.

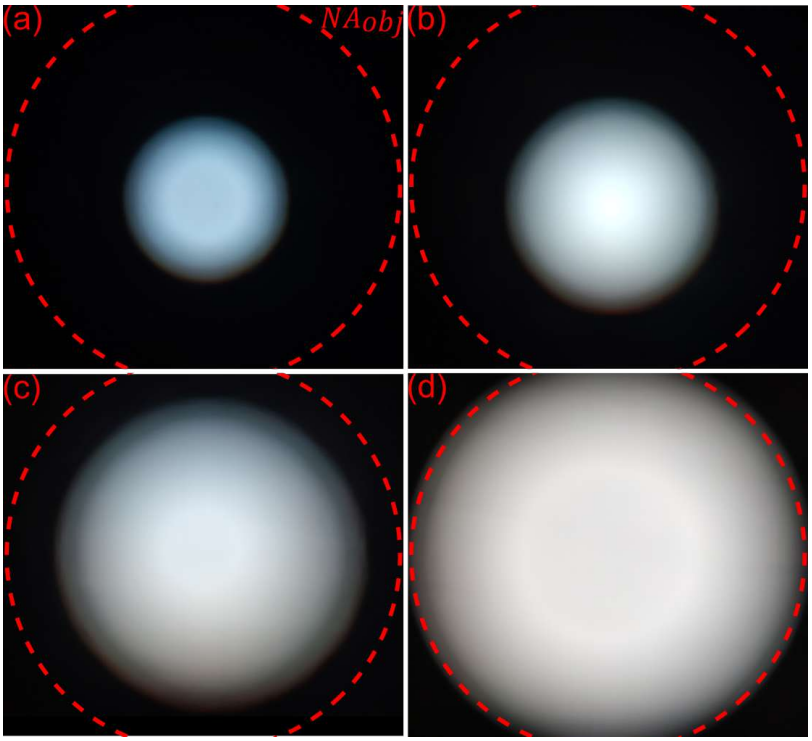

Figure 5.5: Adjusting the illumination NA by varying the diameter of a white circular pattern on the OLED display to match the NA of the objective lens. The dotted red circles represent the objective NA. (a) $NA_{ill} = 0.3NA_{obj}$, (b) $NA_{ill} = 0.45NA_{obj}$, (c) $NA_{ill} = 0.8NA_{obj}$, (d) $NA_{ill} \cong 1.0NA_{obj}$.

three primary colors on the display panel. The radius of these circular patterns is adjusted to match the NA of the objective lens, which is similar to the adjustment of the condenser diaphragm in a conventional laboratory microscope. This has been illustrated thoroughly in the figure 5.5. The illumination characteristics of the OLED display have been studied using a compact CCD spectrometer (CCS200, Thorlabs). Figure 5.6(a) and (b) represents the characteristic emission spectra of the OLED while considering the white light (400-700 nm) and other three primary colors, blue (460 nm), green (525 nm), and red (612 nm), recorded by the spectrometer. For BF microscopic imaging, a white circular pattern has been created on the display panel, shown in figure 5.2(c). Other pixels are turned off outside this circle. For DF imaging, a complementary dark circle on the display panel is patterned as shown in figure 5.2(c). The pixels inside the circle are set to dark while the pixels outside it are set to white. The diameter of the dark circle has been set just greater than the NA of the objective lens. This would prevent the zero-order illuminating beam from entering the objective lens. This technique is similar to adding a DF aperture stop to the condenser diaphragm in a conventional microscope. Another very important and most widely used microscopic technique is fluorescence microscopy, which allows contrast visualization of specific target elements in the sample. This imaging mode can be realized on our PISM system by displaying colored circular patterns of desired

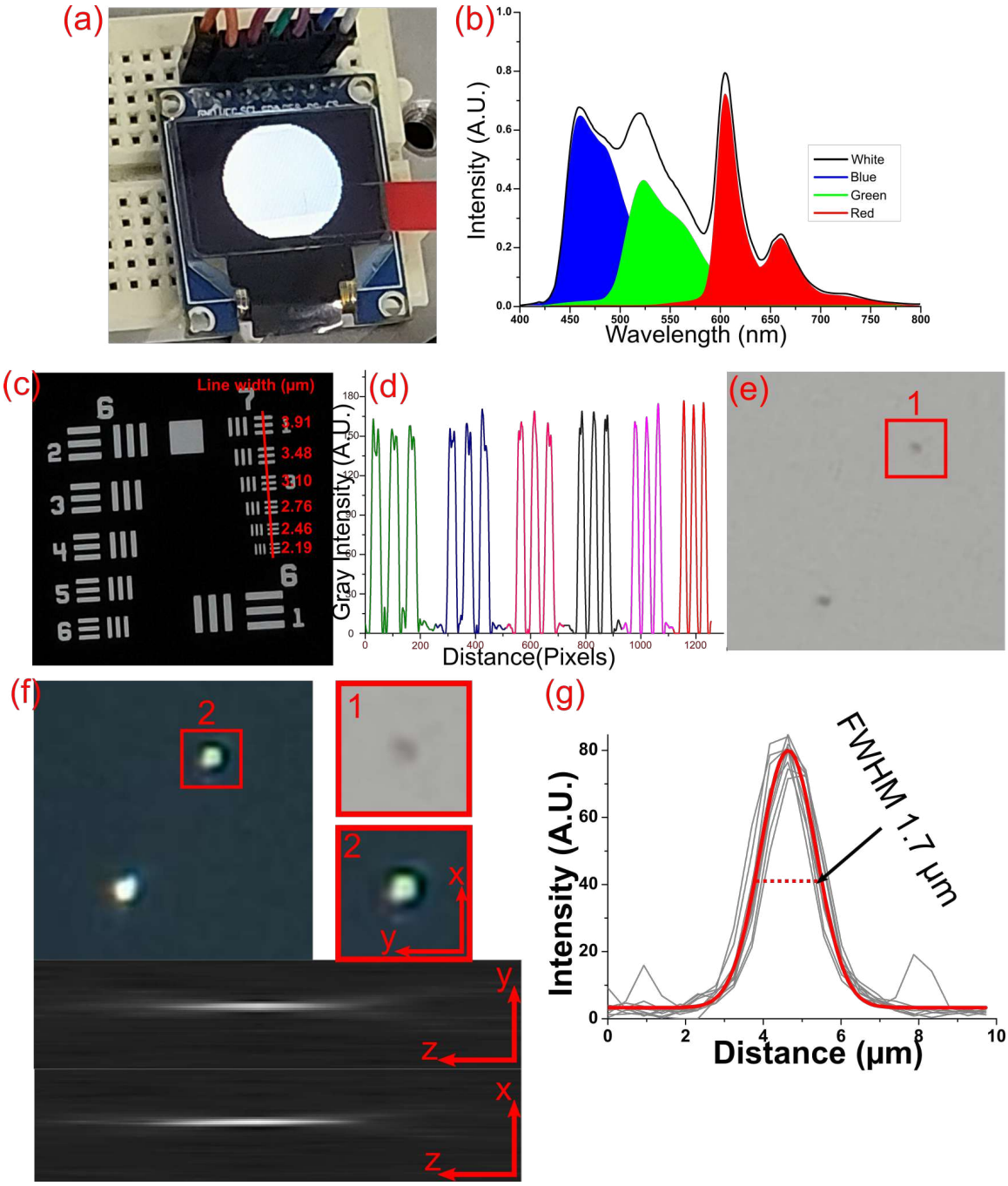

Figure 5.6: Characterization of the PISM system. (a) The photograph of the OLED display panel showing a bright circle, employed in the PISM as an illumination source, (b) Spectral response of the OLED display when a white, blue, green, and red circle is displayed on the panel, (c) image of a USAF-1951 resolution test target acquired by the PISM, showing spatial resolution of the microscopic system up to Group 7 Element 6 (2.19 μm), (d) represents the intensity profile of the entire Group 7 indicated in red line in fig.(c), (e) and (f) show the BF and DF image of 1 μm diameter microbeads captured by the PISM. (f) bottom panel represents the x-y, y-z and x-z views of the point-spread function reconstructed for the imaged micro bead labeled as 2 in the figure and (g) Measurement of full width at half maximum (FWHM) of the PSF in lateral direction by taking average values of 10 microbeads within the FoV of the PISM.

wavelength. A bandpass optical filter is placed in the detection path to remove the excitation wavelength. As the OLED display can produce and adjust different colors and intensity level of the emitting light, these features offer another advantage of developing other color contrast imaging mode such as RI mode of imaging. In this technique, rich color can be rendered to a colorless specimen against another contrasting color background. Both the central and the outer circles in RI are of different colors. These are chosen based on the requirements of the sample to maximize the contrast enhancement. The RI mode of imaging can be visualized as a multiplexing of BF and DF imaging since both the central and the surrounding hollow circles of light produce the image of the specimen simultaneously. Another widely used microscopic mode to visualize unstained colorless specimen is phase-contrast imaging. For the designed PISM system, this mode of imaging can be achieved by using two complementary semicircular illumination patterns on the OLED panel and capture two different images I_1 and I_2 for the same region of the specimen. The captured images contain phase information of the specimen along the specific axis depending on the orientation of the semicircles. The DPC information can be retrieved by taking a normalized difference of the images. Following equation has been used to produce the final DPC image [3]:

$$DPC(I_{DPC}) = \frac{I_1 - I_2}{I_1 + I_2} \tag{5.1}$$

where, I_1 and I_2 are the intensities of the images for either left and right or top and bottom semicircular optical illuminations acquired by the PISM system. Polarized mode of imaging has also been realized with the PISM system by adding two polarizers in cross orientation position. One polarizer has been mounted in between the OLED display and the specimen slide while the other one was placed between the internal lens of the phone and the external objective lens. These can be coupled to the designed PISM system as a plug-and-play tool.

5.3 Materials and methods

5.3.1 Fabrication and alignment of the PISM

The front camera lens of iPhone 7 has been removed gently from its replacement part using a tweezer without scratching it and subsequently used as an objective lens for the PISM. The electronic components SSD1331 SPI (Serial Peripheral Interface) OLED display module, Arduino Nano microcontroller board, and PCB (printed circuit board) have been acquired from online shopping store (www.amazon.in). The OLED display and the microcontroller have been soldered on a PCB, and the assembly has been connected to the phone's battery through USB-OTG protocol. All the

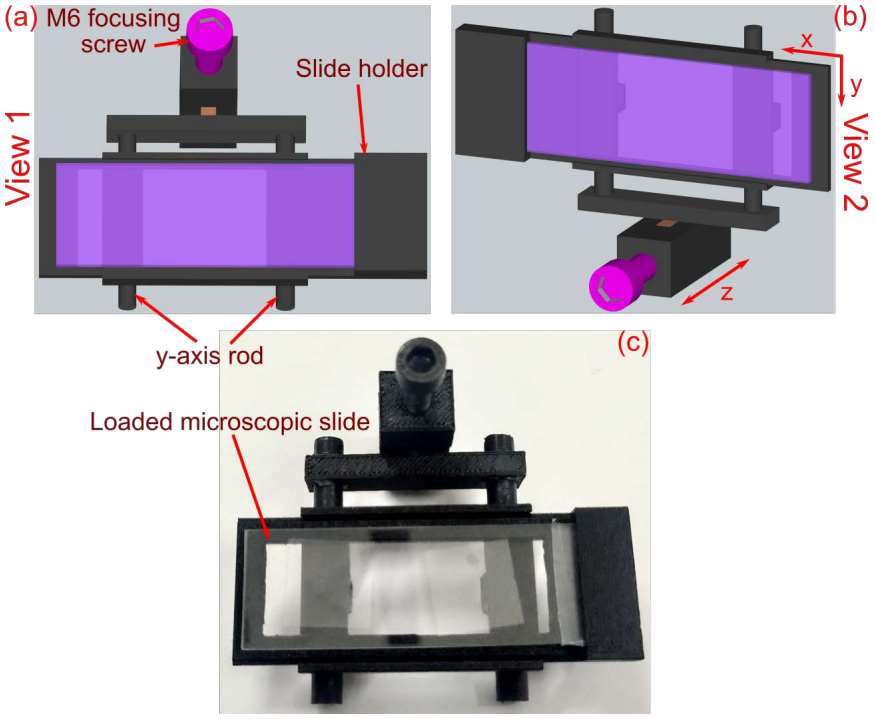

Figure 5.7: 3D-printed XYZ translational stage of the PISM designed to hold a conventional microscopic slide of dimension 75 mm × 25 mm × 1 mm. (a), (b) 3D rendering of the stage in two different views. (c) 3D-printed stage loaded with a sample slide.

components have been rigidly fixed within a 3D-printed chassis. The 3D rendering and photo image of the assembled system are shown in figure 5.2(d) and (e) respectively. A 3D-printed XYZ translational stage has also been incorporated within the chassis to displace and focus the specimen in the respected axes. The 3D visualization and assembled stage are shown in figure 5.7. To make the smooth movement of the sample stage, lubricant (e.g., grease) has been applied to it. The dimension of the designed PISM system is measured to be 80 mm × 45 mm × 45 mm, and the net weight of the setup was found to be ∼96 gm, excluding the phone.

Alignment of the optical setup is critical for reliable operation of the PISM system. The displayed patterns on the OLED must be aligned with the optical axis of the camera lens of the phone and the imaging optics of the setup. One can easily achieve this condition by displaying circles of different diameters on the OLED panel and capturing the patterns by the phone. The position of the pattern on the panel can be adjusted by using the Serial USB Terminal application. For fine focusing on the specimen, the z-axis of the sample stage and the auto-focus adjustment feature of the phone camera application can be used.

5.3.2 Image acquisition and analysis

The built-in camera application of the phone can directly capture the microscopic images upon loading the specimen slide on the sample holder in the PISM system. The phone's camera application provides an advanced control on imaging parameters such as ISO (gain), exposure time, focus, and white balance. A smaller ISO (200-400) has been set to obtain a better signal-to-noise ratio. Exposure time has been maintained between 125 milliseconds to 4 seconds, depending on the imaging mode being considered, specimen types, and dye concentration. For instance, to get enhanced imaging in DF mode, the exposure time was maintained approximately 1 second at an ISO of 200. Usually, smartphone camera applications process raw image data recorded by the CMOS sensor using its internal data processing algorithm and save it in 24-bit RGB color images (JPEG compression). This technique, however, is not suitable for precise quantitative application where maximum raw data acquired by the sensor is indispensable. In such cases, a third-party application software such as Open Camera (by Mark Harman) can be used to save the raw image data (uncompressed) in DNG (digital negative) format. Using data conversion software programs such as Adobe Camera Raw (in Photoshop), the raw image data can be processed as per the requirement and can be saved in 24-bit color RGB format (e.g., TIFF, PNG). Image analysis parameters such as FoV measurement, cell size measurement, adding of scale bars in the images can be performed using Fiji (ImageJ) software. Also, for retrieval of DPC images, image arithmetic operations can be performed using the same applications.

5.3.3 Sample preparation

To evaluate the imaging performance of the designed programmable multimodal smartphone microscope, various samples have been either acquired or procured from vendors. Fluorescent microbeads of dimension 1 μm and 5 μm (Sigma Aldrich, λ_{ex} = 490 nm, λ_{em} = 525 nm) have been diluted in distilled water (DI), and 10 μL each of sample solution has been dispensed on the microscopic slide for imaging. Starch cells were extracted from a potato using a tweezer and diluted in DI water. Human epithelial cheek cells (HECC) were collected from a volunteer by gently scrubbing the inner surface of the cheek using a cotton swab and subsequently smeared it on a microscopic slide for DF and DPC modes of imaging. Also, a part of HECCs were stained with acridine orange for fluorescence imaging. Cultured sample of *Candida albicans* and blood sample have been acquired from the Molecular Biology and Biotechnology (MBBT) department, and Health center of Tezpur University respectively. *C. albicans* was stained with methylene blue, while the blood sample with Leishman solution for imaging with the designed PISM system. H and E stained nerve tissue

sections slide was procured from ESAW, India.

5.4 Optical characterization of the system

Magnification, resolution and FoV

To obtain the best results from the PISM system, an optimal distance of 15 mm has been maintained between the OLED display module and the specimen slide. The optical magnification of the finite-conjugate system is (the ratio of the phone's internal lens FL = 4.77 mm to the external lens FL = 2.87 mm) $M_o = 1.66\times$. The phone has a screen size of 6.39 inches (diagonally) with an aspect ratio of 19.5:9, and its imaging sensor size is 1/2" (8 mm diagonally). The displayed image would yield a digital magnification of ($M_d = \frac{Size_{screen}}{Size_{sensor}}$) $M_d = 20.3\times$ on the phone's screen.

The lateral resolution of the PISM has been characterized by imaging 1951 USAF resolution test target under BF imaging mode. This is shown in figure 5.6(c) and (d). A group of the target specimen is considered to be resolved if the contrast ($C = \frac{I_{max}-I_{min}}{I_{max}-I_{min}}$, I_{max} represents the maximum intensity of the bars and I_{min} represents the minimum intensity of the background) of its bars both vertical and horizontal, exceeds 10%. The objective lens of the PISM system has a NA = 0.23. This would provide a theoretically achievable diffraction-limited resolution of 1.45 μm ($r_{diff} = \frac{0.61\lambda}{NA}$ λ = 550 nm). Experimentally, under white light illumination, we measure a resolution of 2.19 μm, as it can resolve all the group 7 element 6 bars with a contrast of 100%.

To test the resolution ability further, 1 μm diameter microbeads have been imaged in BF and DF mode of the PISM system. These are shown in figure 5.6(e) and (f). It is important to mention that the imaging of 1 μm beads allows viable measurements below the theoretical resolution limit of the microscopic system. The point spread function (PSF) of the system has been evaluated at varying depths in the DF mode. The bottom panel of figure 5.6(f) shows the PSF of the imaged microbead (labeled as 2 in the same figure) in x-y, y-z and x-z directions. The full width at half maximum (FWHM) of the recorded PSF has also been measured in the lateral direction of 10 microbeads within the FoV. Figure 5.6(g) represents the intensity distribution of the PSF function recorded by the designed PISM system. The red bold line in the figure represents the Gaussian-fitted curve of average lateral intensity distribution of the imaged microbeads. The average FWHM value of the recorded images is found to be $\sim$1.7 μm. The optical resolution of the designed PISM system can thus be said to be 1.7 μm. The FoV of the PISM is measured to be 3118 $\times$ 2452 μm^2.

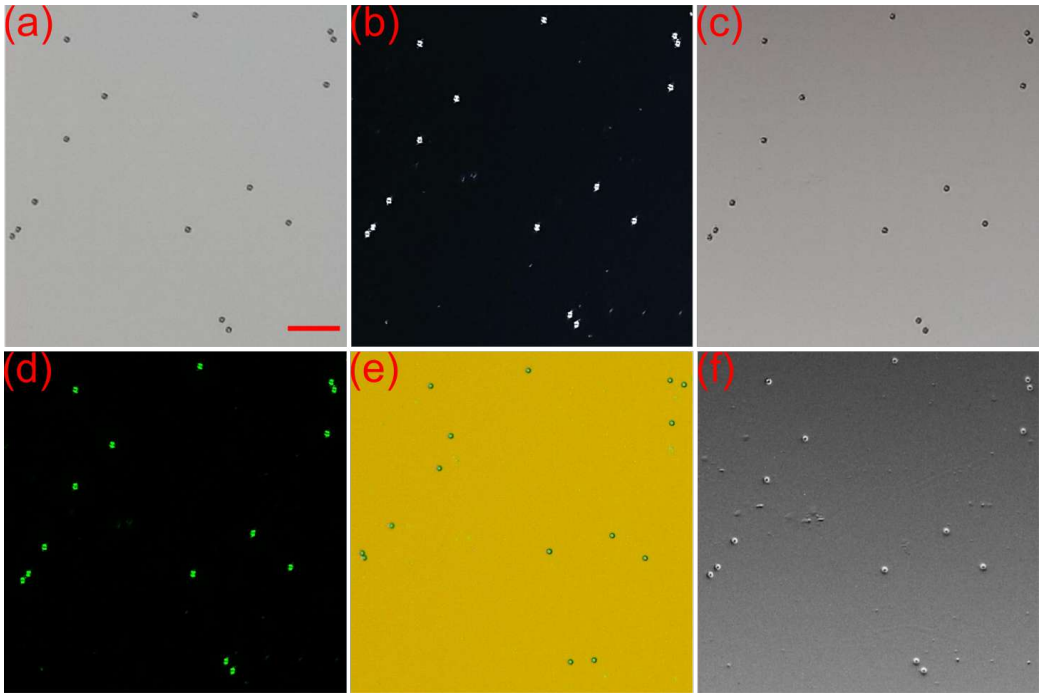

Figure 5.8: Image acquisition by the PISM system under different modes of imaging. Standard 5 μm beads sample have been imaged under (a) BF, (b) DF, (c) OI, (d) fluorescence, (e) RI (yellow/blue), and (f) DPC modes of the PISM. One can clearly see the artifacts and debris that present on the microscopic slide in DF and DPC modes that are not visible in any other modes of imaging. Scale bar is 50 μm.

5.5 Practical applications of the PISM

Different biological specimens have been considered to evaluate the applicability of the multimodal imaging property of the proposed PISM system. Figure 5.8(a), (b), (c), (d), (e), and (f) represent the BF, DF, OI, FI, RI (yellow/blue) and DPC modes of imaging of the standard 5 μm fluorescent beads acquired by the PISM system. The figures clearly indicate that in all the considered modes of imaging, the proposed system captures images with good degree of contrast and structural similarity. Optically translucent biological samples such as HECC cells yield poor contrast to BF mode of imaging while in other modes such as in DF and DPC modes it provides a fairly good contrast images. One can also achieve an enhanced contrast in fluorescence mode upon staining with acridine orange. In the next step of the present study, the performance of the designed PISM system has been evaluated through imaging an optically translucent biological sample- HECC cells. Figure 5.9 represents the BF, DF, DPC and fluorescence mode of imaging of the HECC cells acquired by the PISM system. For fluorescence mode, the HECC cells were stained with acridine orange (AO). As compared to BF mode, the images captured in DF, DPC and FI modes clearly showed an enhancement in the contrast of the imaging sample. The computation of the DPC images have been graphically illustrated in the figure 5.10.

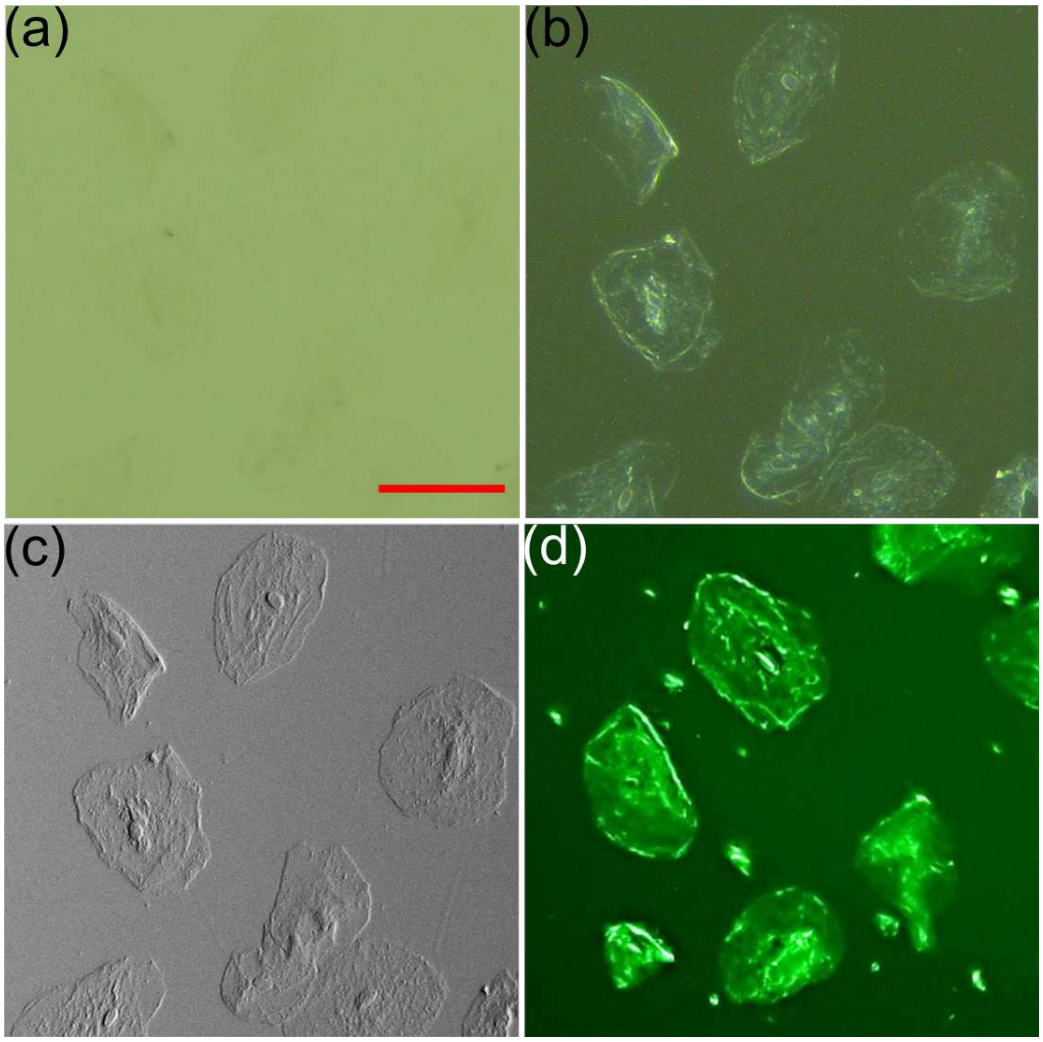

Figure 5.9: Applications of the PISM for multimodal imaging of unstained and stained HECC cells. Zoomed-in image of the unstained HECC cells under (a) BF, (b) DF, (c) DPC, and (d) fluorescence image of HECC cells stained with acridine orange dye. Scale bar is 50 μm.

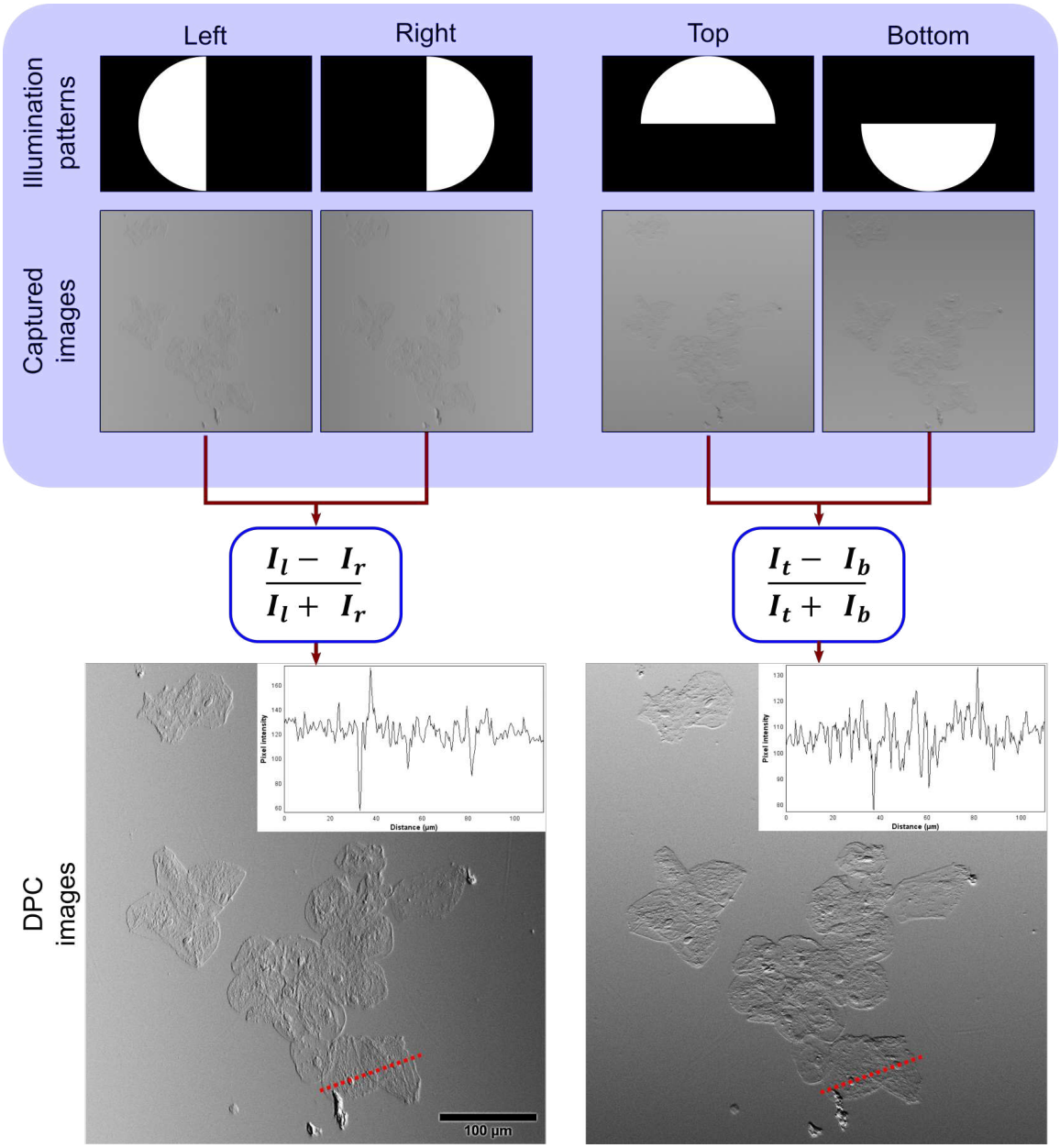

Figure 5.10: Differential phase contrast (DPC) imaging capability of the PISM. The above figures explain the computation for generation of DPC images of unstained HECC cells. Consecutive left, right, top and bottom-half circle illumination patterns are displayed on the OLED display panel and the corresponding images (I_l, I_r, I_t, and I_b)are being recorded respectively. The final phase images are being calculated using the equation (1) along the horizontal axis by taking normalized difference of I_l and I_r, and along the vertical axis by taking normalized difference of I_t and I_b. These are given in the bottom row of the figure. The inset plots of the DPC images represent the intensity fluctuations of the marked cells along red line. Scale bar is 100 μm.

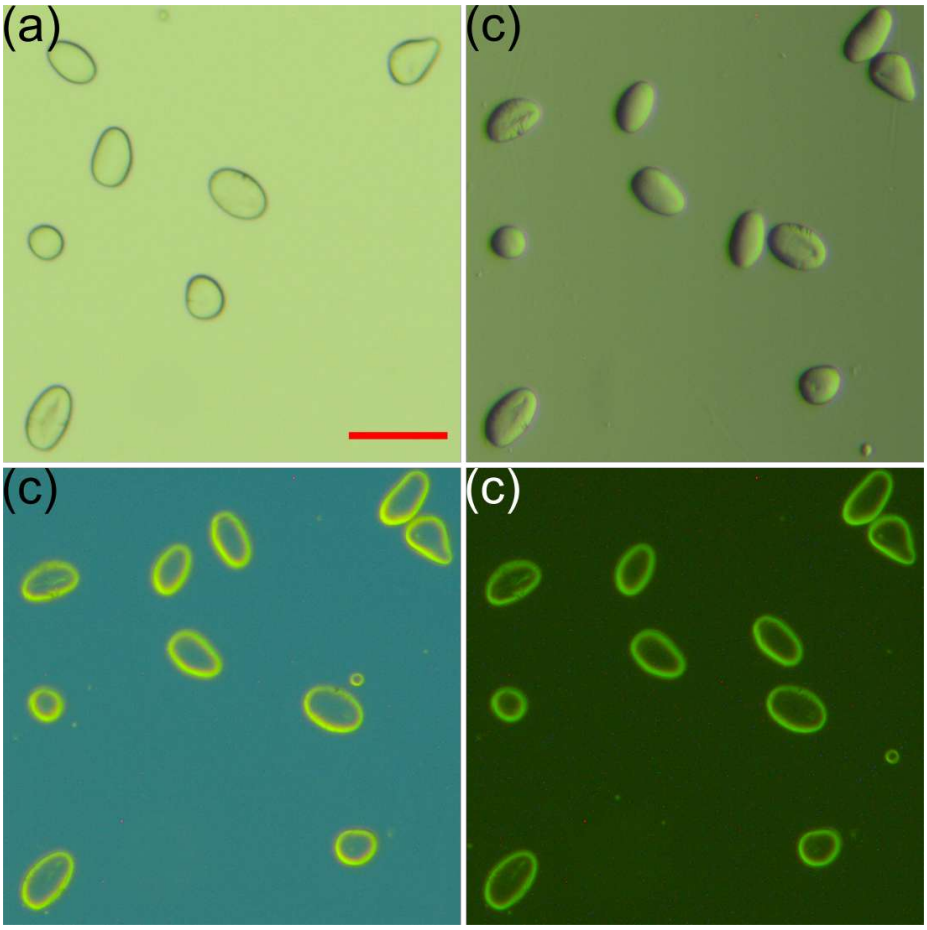

Figure 5.11: Applications of the PISM system for imaging in OI and RI modes. Figure (a) shows the BF image captured by the PISM (b) represents the OI mode of image of the sample while (c) and (d) are the RI images with different color combination (blue/yellow and dark/yellow) in the display panel of the OLED. Scale bar is 50 μm.

To demonstrate the ability of the present PISM system in capturing microscopic images in OI and RI mode, starch cells as specimen has been considered. In these imaging modes, the cells can be stained optically. The illumination patterns that are required on the OLED display for OI and RI modes of imaging have been discussed in the section 5.2.3. Figure 5.11(b) and (c) illustrate the OI and RI (blue/yellow) images of the starch sample captured by the PISM tool. For RI mode, the background color (inner circle) was maintained at blue while the outer circular color was kept yellow. Different RI modes of imaging can be obtained by changing the combination of the primary color patterns on the OLED display. Figure 5.11(d) shows another RI imaging of the starch sample when the background color was maintained at dark and the outer circular pattern was maintained at yellow. For comparison, figure 5.11 also includes the BF image (figure 5.11(a)) of the same region of the starch sample acquired by the PISM system. Clearly, it has been noticed that as compared to the BF mode, the OI and the RI modes of imaging yield a good degree of contrast to the imaging of the test sample.

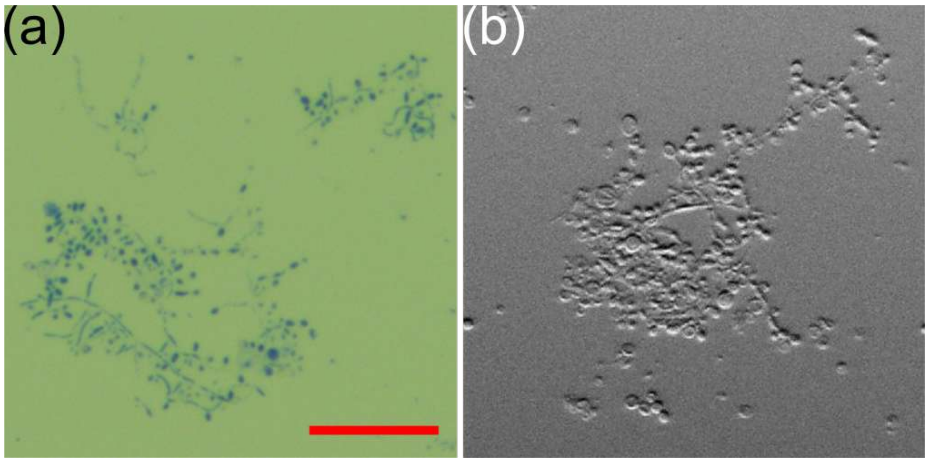

Figure 5.12: Performance evaluation of the PISM system while imaging in DPC mode. (a) and (b) show the BF and DPC images of *C. albicans* respectively when the sample is stained with methylene blue. The hyphae formation in *C. albicans* can be clearly seen in DPC mode. Scale bar is 50 μm.

In the next step of the present study, the performance of the PISM system under DPC mode of imaging has been evaluated. *Candida albicans* has been considered as a test sample for imaging under DPC mode of the designed PISM tool. *Candidiasis* is a fungal infection caused by this species of fungus. Thus, by imaging this fungus can prove the potential applicability of the PISM system for infield diagnostic applications. One of the unique features of the proposed PISM system is that a user can rapidly switch from one mode (e.g. BF mode) to another (e.g. DF, OI, RI or DPC mode) simply by changing the illumination pattern on the OLED display. For DPC mode of imaging, the illumination pattern of the OLED has been maintained as discussed in the section 5.2.3. The optical system captures two separate images under the illumination of two half circular patterns and subsequently performs the intensity distribution computation in accordance with the equation (1) illustrated in section 5.2. Figure 5.12(a) shows the BF imaging of *C. albicans* and (b) represents the DPC mode of imaging of the same region of the sample acquired by the PISM system. Long filamentous hyphae of the fungus can be clearly seen in both the imaging modes of the microscopic system. However, compared to BF mode, with DPC mode one can easily notice a better contrast where detail features of the *C. albicans* sample can be seen. Also, an enhanced imaging contrast of HECCs in DPC mode can be seen while capturing image with the designed PISM system shown in figures 5.9(c) and 5.10.

The applicability of the PISM system has also been demonstrated for histopathology imaging to perform various disease diagnosis and monitoring applications. Figure 5.13(a) and (b) represent the images of the hematoxylin and eosin (H & E) stained tissue section (nerve cell tissue section) under BF imaging acquired by the PISM tool and a laboratory grade microscope (10X, NA 0.25) respectively. The zoomed-in view

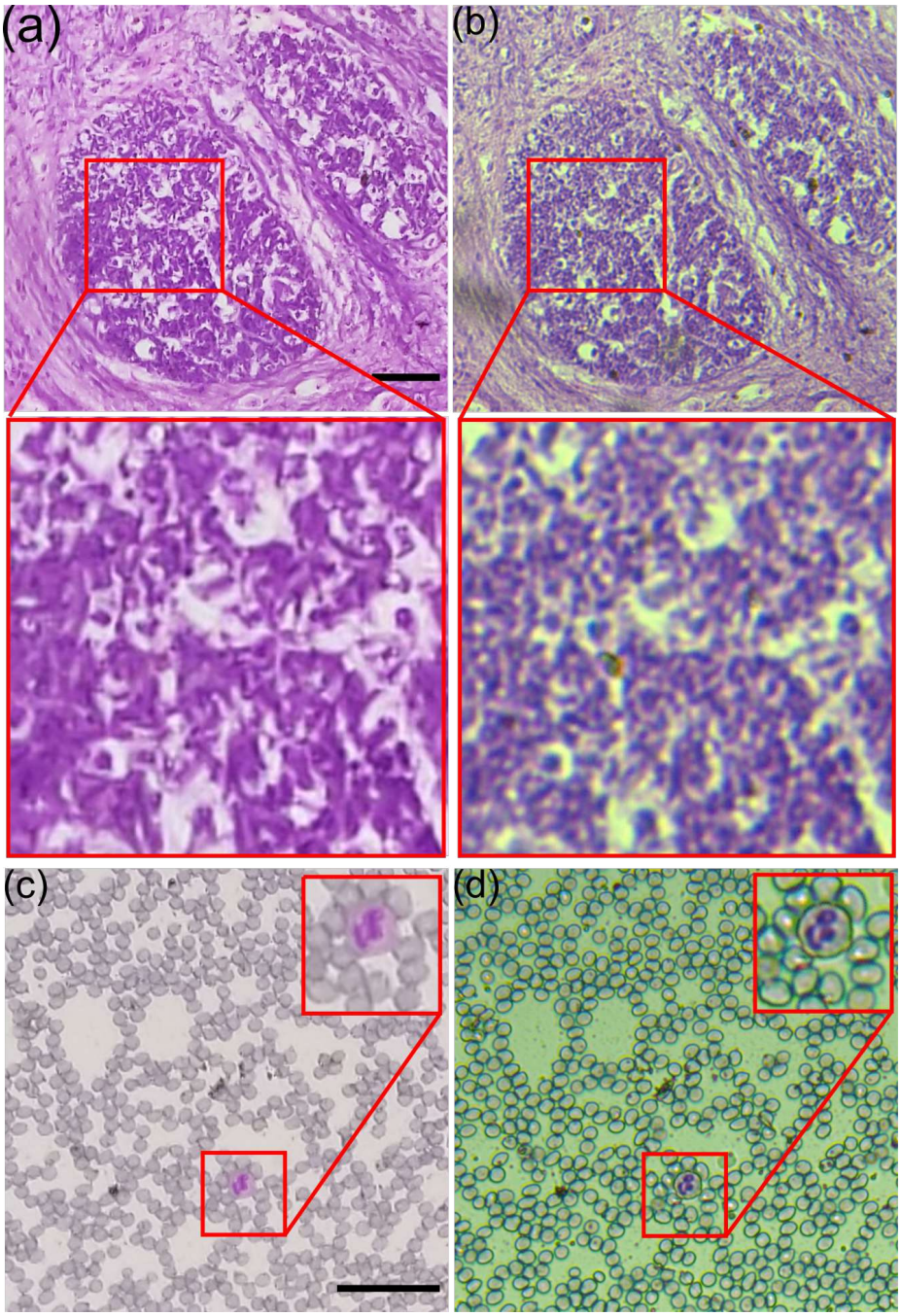

Figure 5.13: Application of the PISM system for histopathology applications. (a) and (b) represent the images of H & E stained nerve cell tissue captured with the PISM and a laboratory microscope (10× objective lens, NA 0.25) respectively under BF mode. The bottom panel in these figures represents the zoomed-in view of the same regions indicated in red squares of (a) and (b). Scale bar is 50 μm. Figure (c) and (d) show the BF images of Leishman stained blood sample acquired by the PISM and the laboratory microscope. Inset figures in (c) and (d) the showed the zoomed-view of the region indicated in squares. Scale bar is 50 μm.

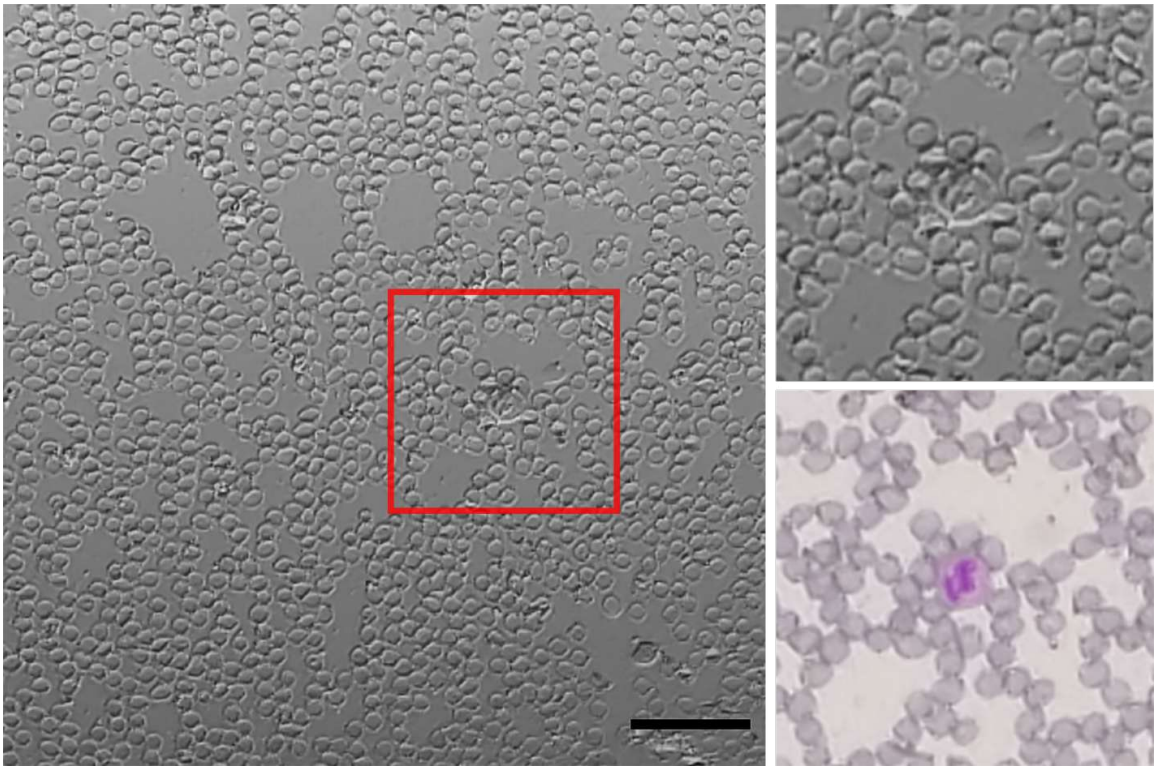

Figure 5.14: Application of the DPC imaging capability of the PISM to histopathology applications by imaging Leishman stained human blood smear. An enlarged view of the red blood cells and white cells indicated in the red box are shown and for comparison to the BF mode of imaging, the same region of interest has been provided on the right hand sight of above figure. Scale bar is 50 μm.

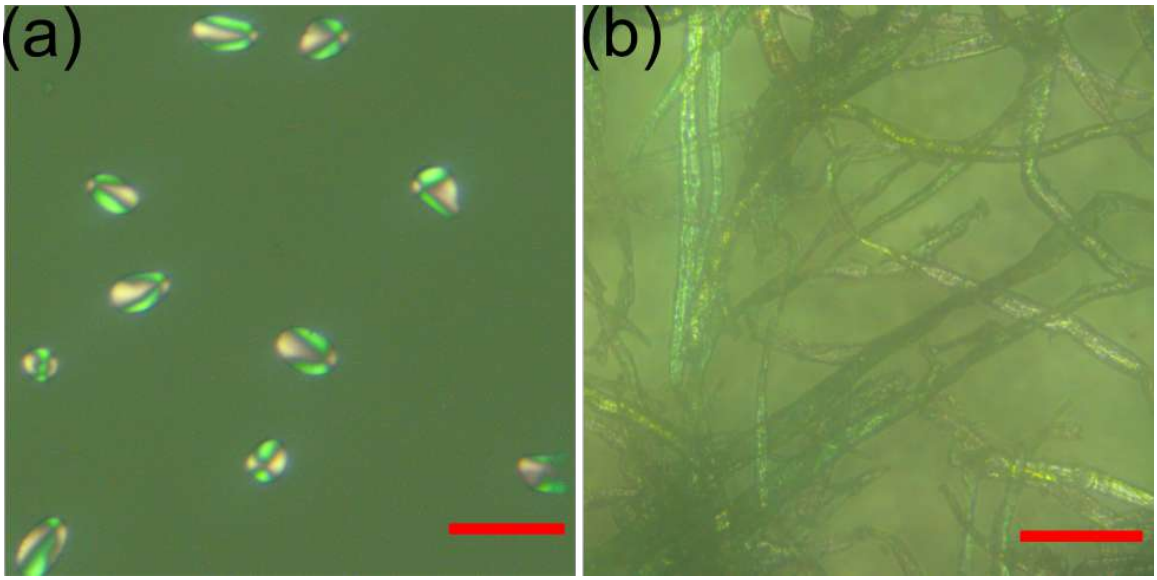

Figure 5.15: Polarized mode of imaging with the designed PISM (a) Polarized imaging of starch sample, and (b) tissue paper. The birefringence natures of the test samples are clearly visible with the PISM system. Scale bars are 50 and 100 μm, respectively.

of the region indicated in red squares in these figures indicates that the performance of the designed tool is at par with that of a laboratory microscope. Also, a stained thin blood smear slide has also been imaged with the PISM system and compared the results with that of a laboratory microscope (10X, NA 0.25). Figure 5.13(c) represents the BF imaging of the sample acquired by the PISM, while (d) represents the imaging of the same region of the sample imaged with the laboratory microscope. The insets of figure 5.13(c), and (d) represent the zoomed-in view of the region of the blood sample captured by the PISM and the standard microscope, respectively. The DPC imaging of the blood sample has also been acquired by the PISM system and shown in the figure 5.14. As compared to BF mode, the DPC mode yields better contrast to the imaging plane. This specific mode of imaging often useful for quantitative analysis such as cell count. It is evident from these figures that the performance of the PISM is as good as the standard tool and thus provides a good degree of reliability of the platform for such applications.

By incorporating additional optical components into the setup, the PISM system can be converted into other mode of imaging. Polarized microscopic tool often requires for imaging of birefringence samples such as crystals and strained non-crystalline substances. Such optical system finds applications in disease diagnosis, biology, and to study rock minerals. In the final step of the present chapter, the working of a polarizing mode of imaging of the designed system has been demonstrated by introducing two polarizers into it. Here, one polarizer has been placed between OLED panel and the specimen while the other has been mounted between the objective lens and the imaging sensor of the phone. Both the polarizers are placed in cross orientation position. Figure 5.15(a) and (b) represent the PI mode of imaging of potato starch and tissue paper specimen captured by the PISM system. The birefringence nature of the starch and tissue paper samples can be clearly seen with the designed setup.

5.6 Discussion

Apart from the seven imaging modalities discussed above, it is also possible to obtain other imaging modes (e.g. 3D tomographic imaging, Fourier ptychography microscopy etc.) with the present imaging setup by exploiting the illumination patterns of the OLED display panel. The OLED as an optical source provides two degrees of freedom for the present multimodal system, viz. intensity of the source can be controlled and peak emission wavelength can be tuned from the smartphone itself. The resolution of the PISM system is pixel-dependent rather than diffraction-limited. It depends on the pixel dimension of the imaging sensor. Though, reasonably high resolution ($\sim$1.7 μm) has been achieved for the present optical system, a more effective

approach to achieving enhanced resolution is implementing $4f$ imaging configuration [19], which is already discussed in chapter 4.

By using the open-source application, imaging modalities can be rapidly switched from one mode to the other without changing the hardware part of the PISM. Though the OLED display screen appears bright for BF and DPC modes of imaging, for other contrast-enhancing imaging such as DF and fluorescence, even a higher intense source is desirable. This issue can be obviated by maintaining a relatively longer exposure time (∼4-8 seconds) while capturing images in DF and fluorescence modes and for BF and DPC modes the exposure time was maintained at few milliseconds (∼125 milliseconds). The net cost involved for development of this versatile imaging platform excluding the smartphone is approximately under $290 (∼INR 22,517) only.

5.7 Summary

In summary, this chapter illustrates the working of a PISM system which is simple, robust, and versatile imaging platform. The designed system can be developed at all skill levels. Different contrast enhancing imaging modalities have been demonstrated on a single optical setup by controlling the illumination pattern on the OLED display panel. The designed PISM system may emerge as advancement in the field of smartphone based multimodal imaging. The cost and size of the device has been reduced drastically while maintaining the flexibility, robustness and performance in all modalities. The OLED display illumination provides a simple generalized solution for issues related to uneven illumination on the specimen due to the use of different micro-objective lenses, which is often encountered in LED-based smartphone microscopic system. For example, use of a phone camera lens as a micro-objective lens in a smartphone microscope offers several important advantages compared to other lenses, such as achieving high FoV with the least aberration at a very low cost. However, with LED as an optical source, the imaging system suffers significant $\cos^{4th}$ vignetting in the final image due to the elimination of light signal at high field angles, thus requires correction of the illumination source [20]. Due to the use of OLED display as an optical source, the present PISM system is free from such issue. The images acquired by the PISM system in different modalities clearly show the reliability and versatility of the platform and its ability to image almost all kinds of samples with a good degree of contrast. The proposed tool could emerge as a promising alternative to the benchtop tools for resource-poor settings, PoC diagnostics, and consumer-health monitoring applications.

References

[1] Boas, D. A., Pitris, C., and Ramanujam, N. *Handbook of biomedical optics*. CRC press, 2016.

[2] Diederich, B., Lachmann, R., Carlstedt, S., Marsikova, B., Wang, H., Uwurukundo, X., Mosig, A. S., and Heintzmann, R. A versatile and customizable low-cost 3d-printed open standard for microscopic imaging. *Nature communications*, 11(1):1–9, 2020.

[3] Guo, K., Bian, Z., Dong, S., Nanda, P., Wang, Y. M., and Zheng, G. Microscopy illumination engineering using a low-cost liquid crystal display. *Biomedical optics express*, 6(2):574–579, 2015.

[4] Ji, N. Adaptive optical fluorescence microscopy. *Nature methods*, 14(4):374–380, 2017.

[5] Dai, B., Jiao, Z., Zheng, L., Bachman, H., Fu, Y., Wan, X., Zhang, Y., Huang, Y., Han, X., Zhao, C., et al. Colour compound lenses for a portable fluorescence microscope. *Light: Science & Applications*, 8(1):1–13, 2019.

[6] Murphy, D. B. *Fundamentals of light microscopy and electronic imaging*. John Wiley & Sons, 2002.

[7] Zuo, C., Sun, J., Feng, S., Hu, Y., and Chen, Q. Programmable colored illumination microscopy (pcim): a practical and flexible optical staining approach for microscopic contrast enhancement. *Optics and Lasers in Engineering*, 78:35–47, 2016.

[8] Ozcan, A. Mobile phones democratize and cultivate next-generation imaging, diagnostics and measurement tools. *Lab on a Chip*, 14(17):3187–3194, 2014.

[9] Ballard, Z. S., Brown, C., and Ozcan, A. Mobile technologies for the discovery, analysis, and engineering of the global microbiome. *ACS nano*, 12(4):3065–3082, 2018.

[10] Vashist, S. K., Luppa, P. B., Yeo, L. Y., Ozcan, A., and Luong, J. H. Emerging technologies for next-generation point-of-care testing. *Trends in biotechnology*, 33(11):692–705, 2015.

[11] Zhang, W., Guo, S., Carvalho, W. S. P., Jiang, Y., and Serpe, M. J. Portable point-of-care diagnostic devices. *Analytical Methods*, 8(44):7847–7867, 2016.

[12] Dong, S., Guo, K., Nanda, P., Shiradkar, R., and Zheng, G. Fpscope: a field-portable high-resolution microscope using a cellphone lens. *Biomedical optics express*, 5(10):3305–3310, 2014.

[13] Aidukas, T., Eckert, R., Harvey, A. R., Waller, L., and Konda, P. C. Low-cost, sub-micron resolution, wide-field computational microscopy using opensource hardware. *Scientific reports*, 9(1):1–12, 2019.

[14] Phillips, Z. F., D'Ambrosio, M. V., Tian, L., Rulison, J. J., Patel, H. S., Sadras, N., Gande, A. V., Switz, N. A., Fletcher, D. A., and Waller, L. Multi-contrast imaging and digital refocusing on a mobile microscope with a domed led array. *PloS one*, 10(5):e0124938, 2015.

[15] Jung, D., Choi, J.-H., Kim, S., Ryu, S., Lee, W., Lee, J.-S., and Joo, C. Smartphone-based multi-contrast microscope using color-multiplexed illumination. *Scientific reports*, 7(1):1–10, 2017.

[16] Kheireddine, S., Perumal, A. S., Smith, Z. J., Nicolau, D. V., and Wachsmann-Hogiu, S. Dual-phone illumination-imaging system for high resolution and large field of view multi-modal microscopy. *Lab on a Chip*, 19(5):825–836, 2019.

[17] Maurer, C., Jesacher, A., Bernet, S., and Ritsch-Marte, M. What spatial light modulators can do for optical microscopy. *Laser & Photonics Reviews*, 5(1): 81–101, 2011.

[18] Agbana, T. E., Diehl, J.-C., van Pul, F., Khan, S. M., Patlan, V., Verhaegen, M., and Vdovin, G. Imaging & identification of malaria parasites using cellphone microscope with a ball lens. *PloS one*, 13(10):e0205020, 2018.

[19] Zhu, W., Pirovano, G., O'Neal, P. K., Gong, C., Kulkarni, N., Nguyen, C. D., Brand, C., Reiner, T., and Kang, D. Smartphone epifluorescence microscopy for cellular imaging of fresh tissue in low-resource settings. *Biomedical optics express*, 11(1):89–98, 2020.

[20] Switz, N. A., D'Ambrosio, M. V., and Fletcher, D. A. Low-cost mobile phone microscopy with a reversed mobile phone camera lens. *PloS one*, 9(5):e95330, 2014.